ELECTRONIC SUPPLEMENTARY INFORMATION

Ground state of the Fe(II)-porphyrin model system corresponds to quintet: A DFT and DMRG-based tailored CC study

Andrej Antalík, Dana Nachtigallová, Rabindranath Lo, Mikuláš Matoušek, Jakub Lang, Örs Legeza, Jiří Pittner, Pavel Hobza and Libor Veis

Computational details

All CASSCF, TCCSD, and TCCSD(T) calculations were performed with the ORCA program package.[1] The DMRG calculations for the purposes of DMRG-CASSCF were performed with the Budapest QC-DMRG code[2] and the subsequent accurate DMRG calculations for TCCSD and TCCSD(T) by means of the parallel MOLMPS program.[3] The DFT calculations were performed with the TURBOMOLE program.[4]

The calculations have been performed with the following geometries: **1a** – R_{FeN} match the distances from triplet geometry optimization of FeP; **1b** and **1c** – fully optimized **1** in the triplet and quintet states, respectively. B97-D3 functional[5] and TZVPP basis set[6] has been used for the geometry optimizations and following DFT calculations. For the TCCSD/TCCSD(T) calculations def2-SVP and def2-TZVP[7] basis sets were used with the auxiliary def2-TZVPP/C[8] basis set. In def2-SVP basis, the canonical TCCSD/TCCSD(T) calculations of **1** are feasible and this basis was therefore used to assess the accuracy of the DLPNO approximation, for which we applied the TightPNO settings in ORCA. Nevertheless, the main conclusions of this work are based on calculations performed in the def2-TZVP basis set.[7] All presented calculations are non-relativistic.

Following the works of Li Manni et al.[9,10] three active spaces were selected: CAS(8,12) constructed from 3d, 4s and 4d orbitals of Fe center and $\sigma_{\mathrm{Fe–N}}$, CAS(12,16) containing additional four ring π-orbitals selected according to their single orbital entropies[11–14] and CAS(32,34) containing the complete π-space. The molecular orbitals have been optimized by means of the standard CASSCF for CAS(8,12) and CAS(12,16) or the DMRG-CASSCF[15,16] method for CAS(32,34). For the latter, the bond dimension, which is the main parameter influencing the accuracy of DMRG, was fixed to 1024.

The acquired orbitals were then split-localized,[17] and accurate DMRG calculations employing the dynamical block state selection[18] were performed with the truncation error criterion set to 10^{-6} and the maximum bond dimension set to 8200. These final DMRG energies are presented in the following text as DMRG-CASSCF. In case of the triplet state calculations, which turned out to be more correlated, the maximum bond dimension was reached by DBSS and the actual truncation error was slightly higher, corresponding roughly to 10^{-5}. The active space single and double CC amplitudes have been generated from the aforementioned accurate DMRG calculations and subsequently used in the TCCSD and TCCSD(T) runs. In the following, we denote the TCCSD/TCCSD(T) methods by the abbreviations TCCSD(e,o)/TCCSD(T)(e,o), where the numbers inside the brackets specify the DMRG active space. To avoid the confusion, we would like to note that in some older works, we denoted the DMRG-based TCCSD method as DMRG-TCCSD.

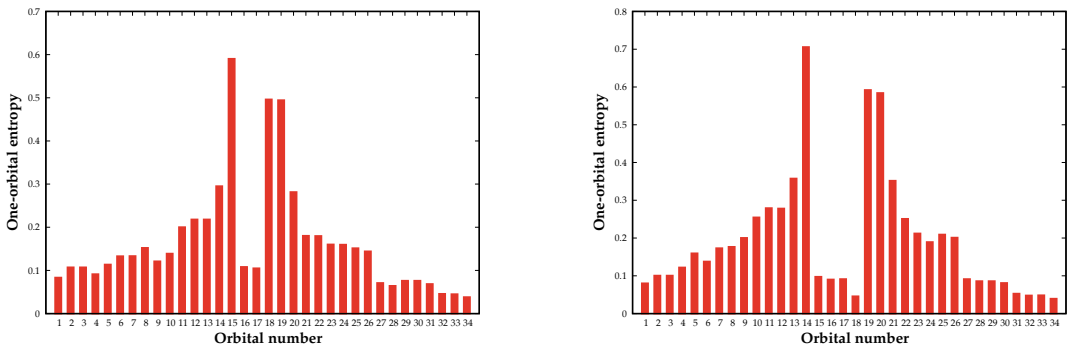

Figure 1: One-orbital entropies from DMRG(32,34) calculation of the triplet (left) and quintet (right) state.

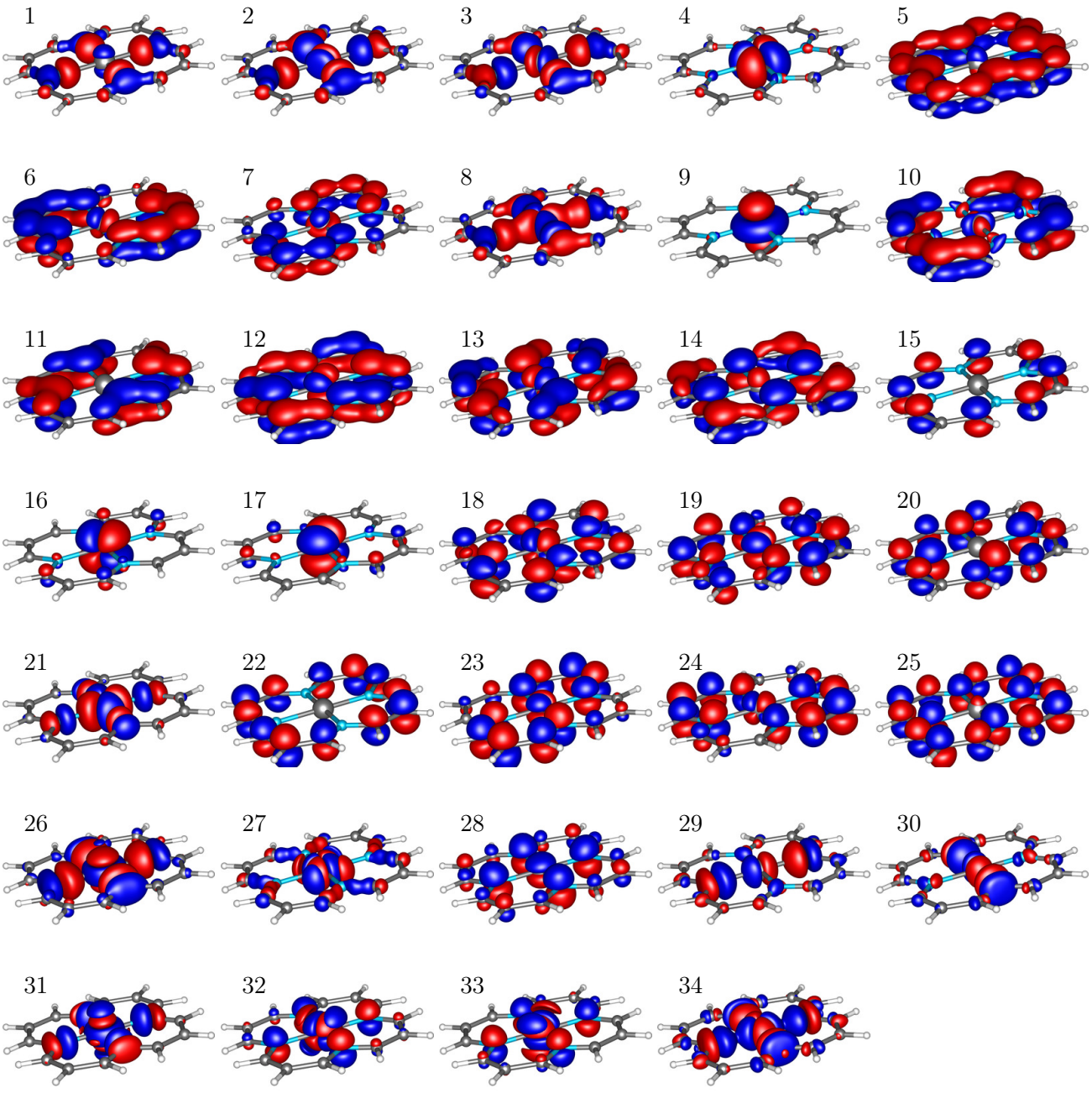

Figure 2: Natural orbitals from DMRG-CASSCF(32,34)/def2-TZVP calculation of the triplet state on **1a**.

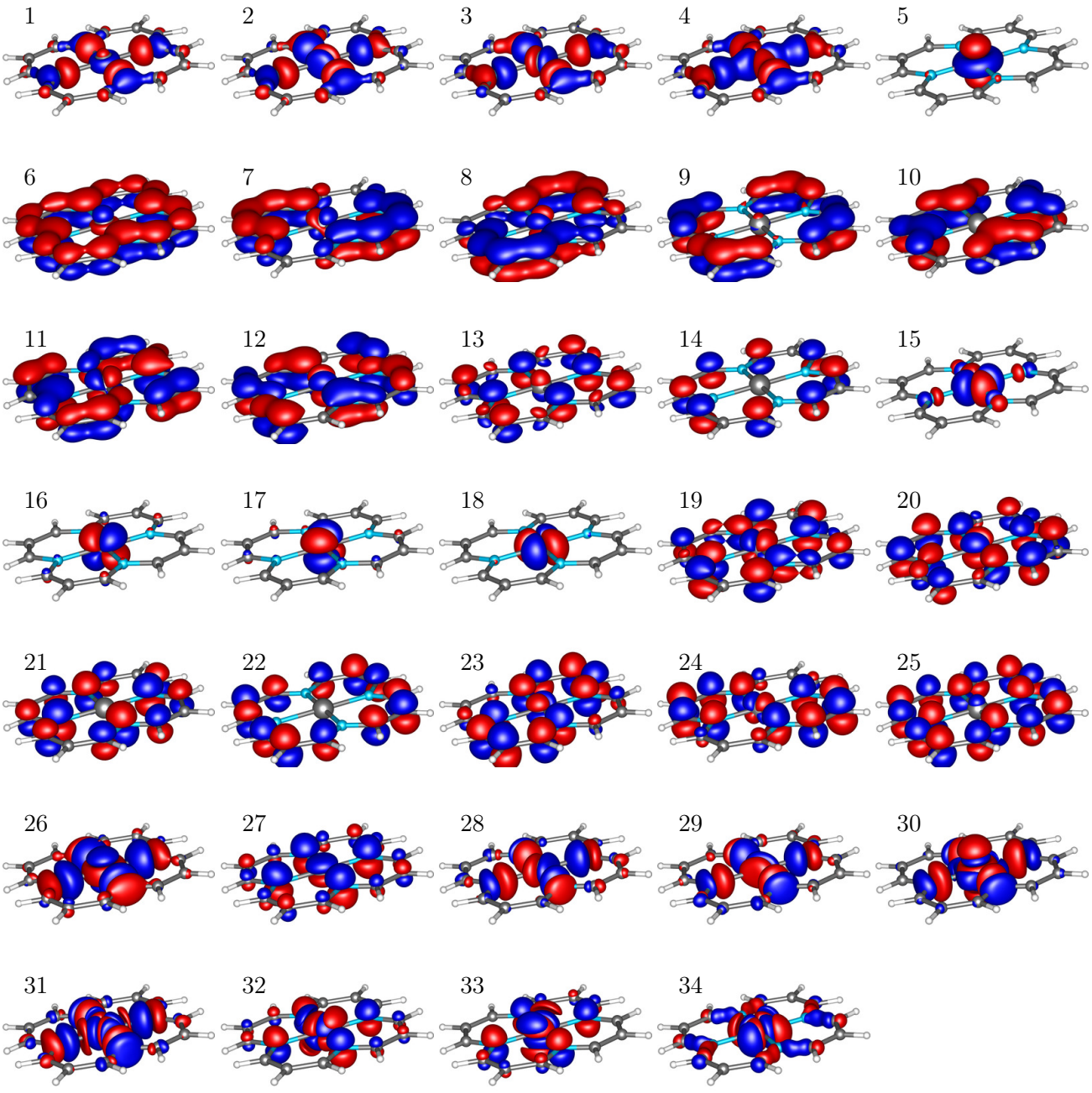

Figure 3: Natural orbitals from DMRG-CASSCF(32,34)/def2-TZVP calculation of the quintet state on **1a**.

Table 1: Relative energies in kcal/mol of different spin states of Fe(II)-porphyrin and Fe(II)-phthalocyanine calculated at B97-D3/def2-TZVPP level. All geometries were optimized specifically for each state at the same level.

	singlet	triplet	quintet
FeP	35.1	0.0	4.5
FePc	32.7	0.0	15.2

Table 2: Accuracy assessment of DLPNO versions of TCCSD and TCCSD(T) with respect to the canonical method in def2-SVP. The canonical and DLPNO energies of FeP model **1** $E + 1940$ in atomic units. Differences between DLPNO and canonical version ΔE_{err} in kcal/mol.

			TCCSD			TCCSD(T)		
CAS	geom.	$2S+1$	can	DLPNO	ΔE_{err}	can	DLPNO	ΔE_{err}
(8,12)	**1a**	3	-3.466399	-3.461605	3.01	-3.586620	-3.578598	5.03
		5	-3.473192	-3.469345	2.41	-3.592151	-3.585165	4.38
	1b	3	-3.505462	-3.501229	2.65	-3.624347	-3.617121	4.53
		5	-3.525479	-3.521328	2.60	-3.643125	-3.636021	4.45
	1c	3	-3.505174	-3.501518	2.29	-3.624203	-3.617803	4.01
		5	-3.547803	-3.544041	2.36	-3.666072	-3.659601	4.06
(12,16)	**1a**	3	-3.479952	-3.476334	2.27	-3.592947	-3.586371	4.12
		5	-3.486586	-3.483339	2.04	-3.597964	-3.591826	3.85
	1b	3	-3.518720	-3.515139	2.25	-3.629978	-3.623607	3.99
		5	-3.538477	-3.534815	2.30	-3.648274	-3.641837	4.04
	1c	3	-3.517667	-3.514309	2.11	-3.628238	-3.622224	3.77
		5	-3.560034	-3.556577	2.17	-3.669452	-3.663340	3.83
(32,34)	**1a**	3	-3.539272	-3.534045	3.28	-3.620836	-3.612188	5.42
		5	-3.543305	-3.537927	3.37	-3.624240	-3.615497	5.48
	1b	3	-3.578319	-3.573427	3.07	-3.658510	-3.650367	5.11
		5	-3.593932	-3.588727	3.26	-3.673696	-3.665162	5.35
	1c	3	-3.576127	-3.571336	3.00	-3.655592	-3.647710	4.94
		5	-3.616008	-3.611176	3.03	-3.695094	-3.687117	5.00

Table 3: The absolute value of energy differences of quintet-triplet gaps between DLPNO and canonical versions of and TCCSD and TCCSD(T) in kcal/mol for different excitations and geometries of FeP model **1** in def2-SVP basis set. Adiabatic gap calculations performed in fully optimized triplet **1b** and quintet geometries **1c**.

	TCCSD			TCCSD(T)		
	CAS(8,12)	CAS(12,16)	CAS(32,34)	CAS(8,12)	CAS(12,16)	CAS(32,34)
$\mathbf{1a}_{\text{vert}}$	0.59	0.23	0.09	0.65	0.27	0.06
$\mathbf{1b}_{\text{vert}}$	0.05	0.05	0.20	0.08	0.04	0.24
adiab.	0.30	0.08	0.04	0.47	0.16	0.10

Table 4: The FeP model **1** energies $E + 1940$ in atomic units. Results for different active spaces and in various basis sets. The CASSCF energies for the largest active space correspond to the DMRG energies obtained by a DMRG calculation from orbitals optimized by DMRG-CASSCF (see Computational Details). The TCCSD and TCCSD(T) energies were obtained by the DLPNO version of the methods.

			def2-SVP			def2-TZVP		
CAS	geom.	$2S+1$	CASSCF	TCCSD	TCCSD(T)	CASSCF	TCCSD	TCCSD(T)
(8,12)	**1a**	3	-0.886588	-3.461605	-3.578598	-1.804012	-4.928912	-5.091471
		5	-0.903920	-3.469345	-3.585165	-1.821258	-4.933315	-5.094495
	1b	3	-0.936200	-3.501229	-3.617121	-1.852420	-4.963201	-5.125573
		5	-0.967032	-3.521328	-3.636021	-1.882908	-4.981797	-5.142654
	1c	3	-0.943239	-3.501518	-3.617803	-1.856259	-4.957341	-5.120104
		5	-0.996546	-3.544041	-3.659601	-1.908779	-4.997301	-5.157307
(12,16)	**1a**	3	-0.928719	-3.476334	-3.586371	-1.846019	-4.945849	-5.102789
		5	-0.946078	-3.483339	-3.591826	-1.862955	-4.949873	-5.105206
	1b	3	-0.977815	-3.515139	-3.623607	-1.894144	-4.980852	-5.135892
		5	-1.008441	-3.534815	-3.641837	-1.924404	-4.997962	-5.151307
	1c	3	-0.983792	-3.514309	-3.622224	-1.896796	-4.971955	-5.126291
		5	-1.036847	-3.556577	-3.663340	-1.949085	-5.012144	-5.164731
(32,34)	**1a**	3	-1.219548	-3.534045	-3.612188	-2.132268	-5.008000	-5.129113
		5	-1.219731	-3.537927	-3.615497	-2.128293	-5.008580	-5.128940
	1b	3	-1.267819	-3.573427	-3.650367	-2.178536	-5.042363	-5.162134
		5	-1.280414	-3.588727	-3.665162	-2.188615	-5.055703	-5.174619
	1c	3	-1.274928	-3.571336	-3.647710	-2.182882	-5.032823	-5.151629
		5	-1.312913	-3.611176	-3.687117	-2.216008	-5.069376	-5.187528

Table 5: The quintet to triplet excitation energies $\Delta E^{\mathrm{Q}\to\mathrm{T}} = E^{\mathrm{T}} - E^{\mathrm{Q}}$ in kcal/mol corresponding to the def2-TZVP basis. Adiabatic calculations performed in fully optimized triplet **1b** and quintet geometries **1c**.

	CAS(8,12)			CAS(12,16)			CAS(32,34)		
	$\mathbf{1a}_{\mathrm{vert}}$	$\mathbf{1b}_{\mathrm{vert}}$	adiab.	$\mathbf{1a}_{\mathrm{vert}}$	$\mathbf{1b}_{\mathrm{vert}}$	adiab.	$\mathbf{1a}_{\mathrm{vert}}$	$\mathbf{1b}_{\mathrm{vert}}$	adiab.
(DMRG-)CASSCF	10.81	19.12	35.34	10.62	18.97	34.45	−2.49	6.32	23.49
DLPNO-TCCSD	2.76	11.66	21.38	2.52	10.73	19.62	0.36	8.36	16.94
DLPNO-TCCSD(T)	1.90	10.71	19.90	1.52	9.67	18.08	−0.11	7.83	15.92

Table 6: The single reference DLPNO-CCSD and CCSD(T) quintet to triplet excitation energies $\Delta E^{\mathrm{Q}\to\mathrm{T}} = E^{\mathrm{T}} - E^{\mathrm{Q}}$ in kcal/mol calculated with the DMRG-CASSCF(32,34) and B3LYP/ROKS orbitals in def2-TZVP basis. Adiabatic calculations performed in fully optimized triplet **1b** and quintet geometries **1c**.

	CASSCF(32,34)			B3LYP/ROKS		
	$\mathbf{1a}_{\mathrm{vert}}$	$\mathbf{1b}_{\mathrm{vert}}$	adiab.	$\mathbf{1a}_{\mathrm{vert}}$	$\mathbf{1b}_{\mathrm{vert}}$	adiab.
DLPNO-CCSD	7.37	15.94	25.82	7.93	16.22	26.09
DLPNO-CCSD(T)	2.69	11.44	20.26	2.75	10.98	20.13

Table 7: Differences in spin gap energies $\Delta E = \Delta E^{\mathrm{Q}\rightarrow\mathrm{T}} - \Delta E^{\mathrm{Q}\rightarrow\mathrm{T}}_{-3\mathrm{s}3\mathrm{p}}$ in kcal/mol with and without the semi-core Fe(3s,3p) correlation for **1a**. The CCSD results taken from Ref.[10]

	def2-SVP		def2-TZVP	
	SD	SD(T)	SD	SD(T)
TCC (can)	−2.7	−2.8		
TCC (DLPNO)	−2.6	−2.6	−3.8	−4.0
CC (can)			−1.2	−1.6

Table 8: The studied geometries of FeP model **1** – **1b** and **1c** were optimized at the B97-D3/def2-TZVPP level and **1a** was taken from Ref.[10]

	1a			**1b**			**1c**		
Atom	x	y	z	x	y	z	x	y	z
Fe	0.000000	0.000000	0.000000	0.000000	0.000000	0.000000	–0.000003	–0.000004	–0.000098
N	1.406727	1.406727	0.000000	1.448270	1.448270	0.000000	1.548142	1.533769	–0.016184
N	–1.406727	1.406727	0.000000	–1.448270	1.448270	0.000000	–1.548640	1.534274	0.016173
N	1.406727	–1.406727	0.000000	1.448270	–1.448270	0.000000	1.548637	–1.534277	0.016177
N	–1.406727	–1.406727	0.000000	–1.448270	–1.448270	0.000000	–1.548141	–1.533769	–0.016178
C	0.000000	3.400142	0.000000	0.000000	3.428797	0.000000	–0.000141	3.446356	–0.000054
C	0.000000	–3.400142	0.000000	0.000000	–3.428797	0.000000	0.000142	–3.446357	–0.000055
C	3.400142	0.000000	0.000000	3.428797	0.000000	0.000000	3.467596	–0.000155	0.000050
C	–3.400142	0.000000	0.000000	–3.428797	0.000000	0.000000	–3.467597	0.000157	0.000047
C	1.222770	2.760387	0.000000	1.221237	2.795853	0.000000	1.254681	2.856378	0.015004
C	–1.222770	2.760387	0.000000	–1.221237	2.795853	0.000000	–1.255157	2.856784	–0.015173
C	1.222770	–2.760387	0.000000	1.221237	–2.795853	0.000000	1.255159	–2.856788	–0.015179
C	–1.222770	–2.760387	0.000000	–1.221237	–2.795853	0.000000	–1.254678	–2.856378	0.015009
C	2.760387	1.222770	0.000000	2.795853	1.221237	0.000000	2.874717	1.253448	–0.013990
C	–2.760387	1.222770	0.000000	–2.795853	1.221237	0.000000	–2.875113	1.253884	0.014133
C	2.760387	–1.222770	0.000000	2.795853	–1.221237	0.000000	2.875108	–1.253881	0.014142
C	–2.760387	–1.222770	0.000000	–2.795853	–1.221237	0.000000	–2.874715	–1.253446	–0.013985
H	0.000000	4.482672	0.000000	0.000000	4.514607	0.000000	0.000007	4.533512	–0.000083
H	0.000000	–4.482672	0.000000	0.000000	–4.514607	0.000000	–0.000008	–4.533513	–0.000089
H	4.482672	0.000000	0.000000	4.514607	0.000000	0.000000	4.554836	0.000010	0.000115
H	–4.482672	0.000000	0.000000	–4.514607	0.000000	0.000000	–4.554837	–0.000012	0.000110
H	2.181081	3.277651	0.000000	2.100989	3.440586	0.000000	2.107723	3.541495	0.049148
H	–2.181081	3.277651	0.000000	–2.100989	3.440586	0.000000	–2.108100	3.542069	–0.049547
H	2.181081	–3.277651	0.000000	2.100989	–3.440586	0.000000	2.108103	–3.542071	–0.049565
H	–2.181081	–3.277651	0.000000	–2.100989	–3.440586	0.000000	–2.107721	–3.541493	0.049154
H	3.277651	2.181081	0.000000	3.440586	2.100989	0.000000	3.554267	2.111248	–0.008046
H	–3.277651	2.181081	0.000000	–3.440586	2.100989	0.000000	–3.554851	2.111619	0.008496
H	3.277651	–2.181081	0.000000	3.440586	–2.100989	0.000000	3.554848	–2.111615	0.008509
H	–3.277651	–2.181081	0.000000	–3.440586	–2.100989	0.000000	–3.554264	–2.111246	–0.008040

References

[1] F. Neese, "The ORCA program system," *Wiley Interdisciplinary Reviews: Computational Molecular Science*, vol. 2, pp. 73–78, June 2011.

[2] Ö. Legeza, L. Veis, and T. Mosoni, "Qc-dmrg-budapest, a program for quantum chemical dmrg calculations."

[3] J. Brabec, J. Brandejs, K. Kowalski, S. Xantheas, Ö. Legeza, and L. Veis, "Massively parallel quantum chemical density matrix renormalization group method," *arXiv e-prints*, p. arXiv:1907.13466, 2020.

[4] "TURBOMOLE V7.3 2018, a development of University of Karlsruhe and Forschungszentrum Karlsruhe GmbH, 1989-2007, TURBOMOLE GmbH, since 2007; available from `http://www.turbomole.com`."

[5] S. Grimme, "Semiempirical GGA-type density functional constructed with a long-range dispersion correction," *Journal of Computational Chemistry*, vol. 27, no. 15, pp. 1787–1799, 2006.

[6] A. Schäfer, C. Huber, and R. Ahlrichs, "Fully optimized contracted gaussian basis sets of triple zeta valence quality for atoms li to kr," *The Journal of Chemical Physics*, vol. 100, pp. 5829–5835, Apr. 1994.

[7] F. Weigend and R. Ahlrichs, "Balanced basis sets of split valence, triple zeta valence and quadruple zeta valence quality for h to rn: Design and assessment of accuracy," *Physical Chemistry Chemical Physics*, vol. 7, no. 18, p. 3297, 2005.

[8] A. Hellweg, C. Hättig, S. Höfener, and W. Klopper, "Optimized accurate auxiliary basis sets for RI-MP2 and RI-CC2 calculations for the atoms rb to rn," *Theoretical Chemistry Accounts*, vol. 117, pp. 587–597, Jan. 2007.

[9] G. L. Manni and A. Alavi, "Understanding the mechanism stabilizing intermediate spin states in fe(II)-porphyrin," *The Journal of Physical Chemistry A*, vol. 122, pp. 4935–4947, Mar. 2018.

[10] G. L. Manni, D. Kats, D. P. Tew, and A. Alavi, "Role of valence and semicore electron correlation on spin gaps in fe(II)-porphyrins," *Journal of Chemical Theory and Computation*, vol. 15, pp. 1492–1497, Jan. 2019.

[11] O. Legeza and J. Sólyom, "Optimizing the density-matrix renormalization group method using quantum information entropy," *Physical Review B*, vol. 68, Nov. 2003.

[12] J. Rissler, R. M. Noack, and S. R. White, "Measuring orbital interaction using quantum information theory," *Chemical Physics*, vol. 323, pp. 519–531, Apr. 2006.

[13] G. Barcza, O. Legeza, K. H. Marti, and M. Reiher, "Quantum-information analysis of electronic states of different molecular structures," *Physical Review A*, vol. 83, Jan. 2011.

[14] C. J. Stein and M. Reiher, "Automated selection of active orbital spaces," *Journal of Chemical Theory and Computation*, vol. 12, pp. 1760–1771, Mar. 2016.

[15] D. Zgid and M. Nooijen, "The density matrix renormalization group self-consistent field method: Orbital optimization with the density matrix renormalization group method in the active space," *The Journal of Chemical Physics*, vol. 128, p. 144116, Apr. 2008.

[16] D. Ghosh, J. Hachmann, T. Yanai, and G. K.-L. Chan, "Orbital optimization in the density matrix renormalization group, with applications to polyenes and $^{\beta}$-carotene," *The Journal of Chemical Physics*, vol. 128, p. 144117, Apr. 2008.

[17] R. Olivares-Amaya, W. Hu, N. Nakatani, S. Sharma, J. Yang, and G. K.-L. Chan, "The ab-initio density matrix renormalization group in practice," *The Journal of Chemical Physics*, vol. 142, p. 034102, Jan. 2015.

[18] O. Legeza, J. Röder, and B. A. Hess, "Controlling the accuracy of the density-matrix renormalization-group method: The dynamical block state selection approach," *Physical Review B*, vol. 67, Mar. 2003.